Nanostructural and Geochemical Features of the Jurassic Isocrinid Columnal Ossicles

Authors: Stolarski, Jarosław, Gorzelak, Przemysław, Mazur, Maciej, Marrocchi, Yves, and Meibom, Anders

Source: Acta Palaeontologica Polonica, 54(1) : 69-75

Published By: Institute of Paleobiology, Polish Academy of Sciences

URL: https://doi.org/10.4202/app.2009.0108

Nanostructural and geochemical features of the Jurassic isocrinid columnal ossicles

JAROSŁAW STOLARSKI, PRZEMYSŁAW GORZELAK, MACIEJ MAZUR, YVES MARROCCHI, and ANDERS MEIBOM

Stolarski, J., Gorzelak, P., Mazur, M., Marrocchi, Y., and Meibom, A. 2009. Nanostructural and geochemical features of the Jurassic isocrinid columnal ossicles. *Acta Palaeontologica Polonica* 54 (1): 69–75.

Calcite isocrinid ossicles from the Middle Jurassic (Bathonian) clays in Gnaszyn (central Poland) show perfectly preserved micro- and nanostructural details typical of diagenetically unaltered echinoderm skeleton. Stereom pores are filled with ferroan calcite cements that sealed off the skeleton from diagenetic fluids and prevented structural and geochemical alteration. In contrast with high-Mg calcite skeleton of modern, tropical echinoderms, the fossil crinoid ossicles from Gnaszyn contain only 5.0–5.3 mole% of $MgCO_3$. This low Mg content can be a result of either a low temperature environment (ca. 10°C) and/or low Mg/Ca seawater ratio. Both conditions have been proposed for the Middle Jurassic marine environment. Occurrence of Mg-enriched central region of stereom bars of Jurassic columnal ossicle of *Chariocrinus andreae* is consistent with the concept of magnesium ions involvement in earliest growth phases of calcium carbonate biominerals.

Key words: Echinodermata, Crinoidea, calcite, nanostructure, geochemistry, AFM, NanoSIMS, Jurassic.

Jarosław Stolarski [stolacy@twarda.pan.pl], and Przemysław Gorzelak [przemyslaw.gorzelak@gmail.com], Institute of Paleobiology, Polish Academy of Sciences, ul. Twarda 51/55, PL-00-818 Warsaw, Poland;
Maciej Mazur [mmazur@chem.uw.edu.pl], Department of Chemistry, Laboratory of Electrochemistry, University of Warsaw, ul. Pasteura 1, PL-02-093 Warsaw, Poland;
Yves Marrocchi [marrocchi@mnhn.fr] and Anders Meibom [meibom@mnhn.fr], Muséum National d'Histoire Naturelle, Laboratoire d'Etude de la Matiere Extraterrestre, USM 0205 (LEME), Case Postale 52, 61 rue Buffon, 75005 Paris, France.

Introduction

Representatives of all echinoderm clades i.e., echinoids, holothuroids, ophiuroids, asteroids, crinoids, and a few other extinct groups, form elaborate calcitic (polymorph of calcium carbonate) skeletons composed of numerous ossicles (or plates). Each plate consists of a three-dimensional meshwork of mineral trabeculae called stereom. Stereom is considered an echinoderm synapomorphy and is recognized already in Cambrian stylophorans, the most basal echinoderm clade (Bottjer et al. 2006; Clausen and Smith 2008). Individual skeletal plates behave as single calcite crystals as shown by X-ray diffraction and polarizing microscopy (Donnay and Pawson 1969), however their physico-chemical properties differ significantly from the properties of geologic or synthetic calcites. For example, echinoderm bio-calcite does not show cleavage planes typical of calcite but reveals conchoidal fracture surfaces that reduce the brittleness of the material by dissipating strain energy and deflecting crack propagation (Berman et al. 1988). The unique properties of echinoderm bio-calcite result from intimate involvement of organic molecules in the biomineralization process and their incorporation into the crystal structure. Organic components, mainly various proteins and glycoproteins, constitute 0.10–0.26 wt% of modern echinoderm bio-calcite (Weiner 1985; Wilt 1999) and are incorporated in the skeleton at different structural levels. At the nanoscale, a distinct feature of calcium carbonate biomineral is its composite structure: mineral grains (commonly 30–100 nm in diameter) are closely associated with an organic material. Nanocomposite structure (nanograins 20–100 nm) have also been reported for bio-calcite of echinoderms, i.e., spines of extant echinoids (Oaki and Imai 2006). Fossil calcium carbonate biominerals that are not diagenetically altered also preserve nanocomposite structure (Stolarski and Mazur 2005).

The goal of this work is to describe fine scale structural and geochemical features of fossil crinoid ossicles recovered from the Middle Jurassic (ca. 167 Ma) sediments in Gnaszyn, Poland. These clay deposits are known for their excellent preservation of aragonitic skeletons that are not dissolved or recrystallized as in many other types of sedimentary rocks of the same age. As aragonite is metastable at ambient temperatures and pressures, and easily transforms into calcite, which is a stable $CaCO_3$ polymorph, it can only be preserved if sealed off from pore-water penetration. Preservation of aragonite fossils at Gnaszyn suggests that crinoid bio-calcite

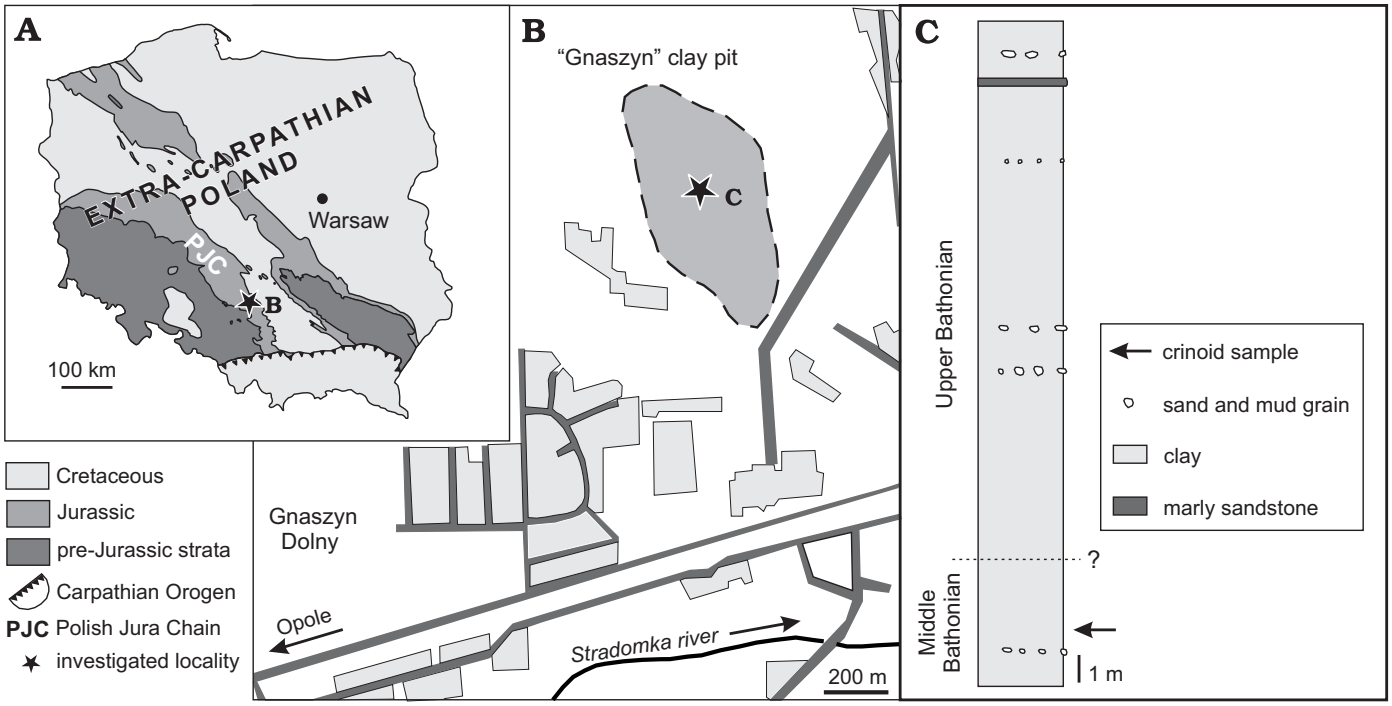

Fig. 1. **A**. Simplified map of Poland with position of investigated Gnaszyn locality. **B**. Enlargement of Gnaszyn area with a clay pit from which crinoid samples were collected (modified after Zatoń et al. 2006). **C**. Stratigraphic column of the Bathonian deposits at Gnaszyn clay pit (modified after Majewski 2000).

might also preserve original structural and geochemical signatures. Note that modern crinoids form magnesium-rich calcite that is also susceptible to diagenesis.

Institutional abbreviation.—GIUS, Faculty of Earth Sciences of the University of Silesia, Poland.

Materials and methods

Materials.—The fossil crinoids were collected from an active clay pit at Gnaszyn Dolny (abbreviated "Gnaszyn") approximately 10 km southwest of Częstochowa (Fig. 1) in Polish Jura Chain of south-central Poland. The sedimentary rocks exposed at Gnaszyn are represented mainly by dark-grey calcareous silty clays, occasionally with levels of sideritic concretions and are dated as Middle Bathonian (*Tulites subcontractus* and *Morrisiceras morrisi* Chrones) and Upper Bathonian (*Procerites hodsoni* Chron = Bremeri and early *Prohecticoceras retrocostatum* Chron in Submediterranean zonation); see Majewski 1997; Zatoń et al. 2006; Matyja and Wierzbowski 2000, 2006. Both the clays and the sideritic concretions are rich in fossils that include bivalves, gastropods, ammonites with preserved aragonitic skeleton as well as belemnites, crustaceans, and echinoderms (Gedl et al. 2003, 2006). Columnals and pluricolumnals of crinoids are the most frequent echinoderm remains at this locality (Salamon and Zatoń 2007). Many of them are dark (black) in color whereas light (beige) columnals represent ca. 10% of the collection. Two columnals from the Middle Bathonian clays of Gnaszyn were examined in more detail: (i) stellate and beige in color columnal of *Chariocrinus andreae* (Desor, 1845) (Fig. 2A), and (ii) circular and dark columnal of *Balanocrinus berchteni* Hess and Pugin, 1983 (Fig. 2B).

Methods.—Atomic Force Microscopy (AFM) was performed with a MultiMode Nanoscope IIIa (Digital Instruments, Veeco), following procedures described in Stolarski and Mazur (2005). Standard silicone nitride cantilevers were used for measurements in contact mode. The polished samples were then etched in 1% ammonium persulfate in McIlvain buffer (pH = 8) for 10 min., followed by rinsing in deionized water and drying. Trace element analyses were performed with the Cameca NanoSIMS N50 at the Muséum National d'Histoire Naturelle in Paris, following procedures described in Meibom et al. (2004, 2008). The samples were polished to 0.25 μm diamond finish then Au-coated. Using a primary beam of O^-, secondary ions of $^{24}Mg^+$, $^{44}Ca^+$, and $^{88}Sr^+$ were sputtered from the sample surface and detected simultaneously (multicollection-mode) in electron-multipliers at a mass-resolving power of ~4500 (M/DM). At this mass-resolving power, the measured secondary ions are resolved from potentially interferences. Data were obtained from a pre-sputtered surface in a series of rasters with the primary ions focused to a spot-size of ~200 nm. The primary beam was stepped across the sample surface with a similar step-size. The measured $^{24}Mg/^{44}Ca$ and $^{88}Sr/^{44}Ca$ ratios were calibrated against analyses of carbonate standards of known composition and against spot elemental analyses performed with a scanning microscope Philips XL-20 coupled with the EDS detector ECON 6 (system EDX-DX4i) at the Institute of Paleobiology, Warsaw, Poland. The BSE detector of the

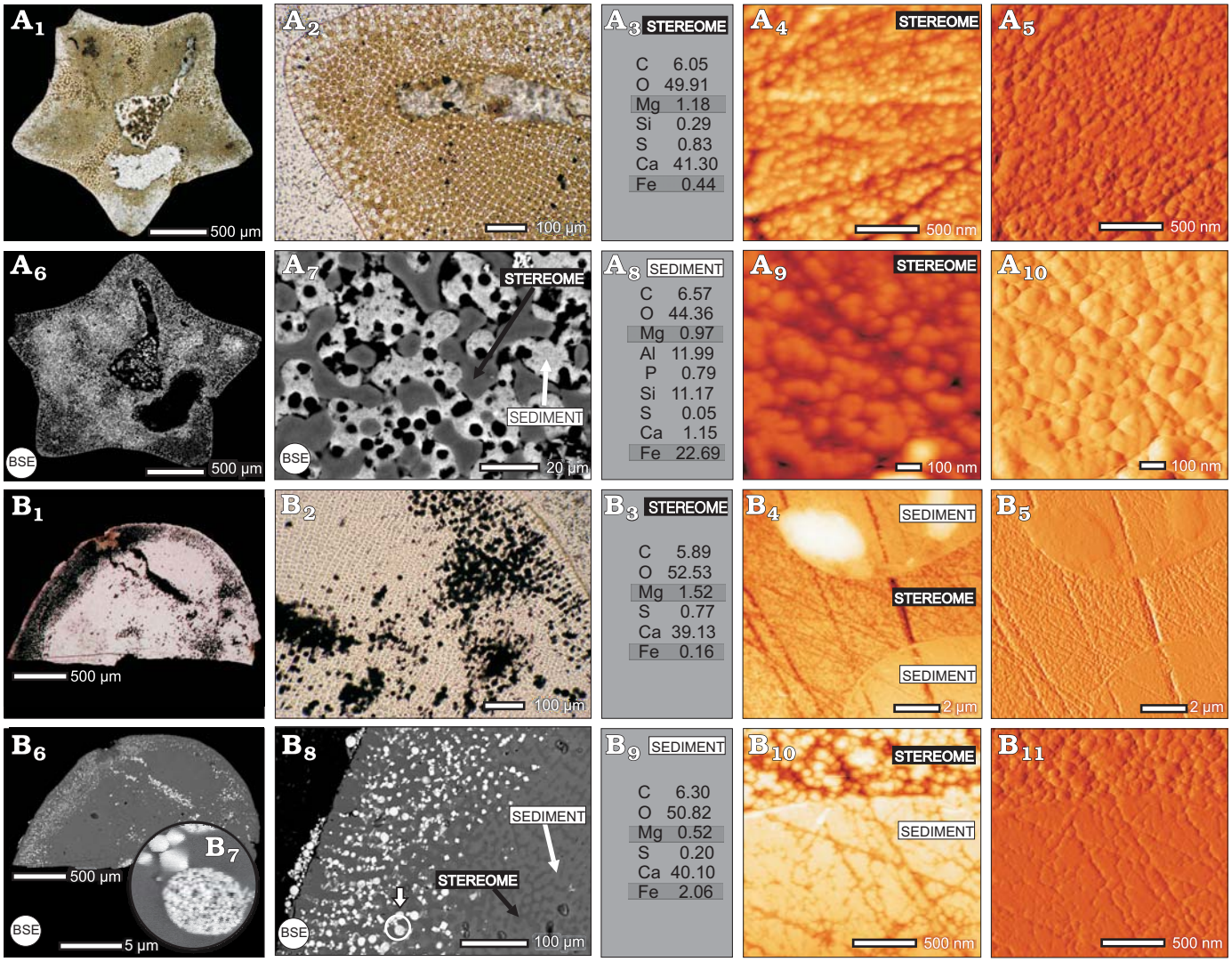

Fig. 2. Micro- and nanostructural organization and basic geochemical characteristics of the Middle Jurassic (Middle Bathonian) isocrinid columnals from Gnaszyn clay pit, Poland. **A**. Transverse section of the columnal (beige in color) of *Chariocrinus andreae* (Desor, 1845), GIUS 8-2570 (A_2 enlargement) in optical microscope (A_1, A_2) and in SEM back-scattered electron (BSE; A_6, A_7) images. Nanogranular organization of the stereom in AFM images (A_4, A_9 height-2D, and A_5, A_{10} deflection images respectively; contact mode; buffered pH = 8, ammonium persulfate 1%, 10 min.). **B**. Slightly oblique section of the columnal (black in color) of *Balanocrinus berchteni* Hess and Pugin 1983, GIUS 8-2510 (B_2 enlargement) in optical microscope (B_1, B_2) and in BSE (B_6–B_8) images. Note a clear border between stereom with distinct nanogranular texture and inter-stereom deposits with more flat surface (parallel lines are polishing scratches); B_4, B_{10} height, and B_5, B_{11} phase images, respectively. BSE mode enhances atomic number contrast; elements with lower atomic numbers appear darker, those with higher atomic numbers appear lighter (e.g., framboidal pyrite grains, B_7). Spot geochemical analyses of the stereom (A_3, B_3) and inter-stereom deposits (A_8, B_9).

Philips XL-20 microscope was used for polished and carbon-coated specimens, allowing to distinguish between material of lower vs. higher molecular density.

Results

Microscale.—In both columnals, the stereom framework is well preserved. The columnal of *Balanocrinus berchteni* Hess and Pugin, 1983 has a circular outline and relatively large, triangular petals. They are encircled by 6–8 marginal crenulae: marginal crenulae are of the same size but distinctly thicker than adradial ones. In the star-shaped columnals of *Chariocrinus andreae* (Desor, 1845), lancet-shaped petals are encircled by well developed crenularium with 12–16 crenulae associate with each petal. In transverse sections of both columnals two distinct regions can be distinguished: (i) petaloid regions built of regular meshwork of galleried type stereom (α-stereom of Roux 1975) and (ii) interpetaloid areas composed of irregular, labyrinthic stereom (β-stereom of Roux 1975). Interstereom spaces in both specimens are infilled with secondary deposits, mostly of ferroan calcite. Secondary deposits developed in the peripheral zone of the *B. berchteni* plate contain numerous framboidal pyrite grains, some of them attaining 5–8 µm in diameter (Fig. 2B_1, B_2, B_6–B_8) that dyes this columnal black. Con-

versely, no pyrite accumulations were observed in interstereom ferroan calcite infilling of light colored plate of *C. andreae*.

Nanoscale.—Calcite stereom skeleton of both columnals consists of nanograins ca. 100 nm in diameter. No distinct variation in the nano-texture was observed in the examined samples. Individual grains have a semicircular outline and are separated from each other by spaces of a few nanometers width (Fig. 2A_4, A_5, A_9, A_{10}, B_4, B_5, B_{10}, B_{11}). Occasionally, larger, up to 300 nm, rounded aggregates of smaller nanograins are visible (Fig. 2A_9, A_{10}). There is a sharp boundary in nanoscale texture between the stereom (distinct nanograins) and interstereom deposits (relatively smooth surface with low value of roughness factor). The stereom surface has deeper grinding scratches and its relief is lower than that of adjacent interstereom deposits that suggests it has a lower hardness.

Geochemistry.—BSE mode images show clear contrast between chemical composition of stereom and interstereom sediment. BSE enhances the atomic number contrast and elements with lower atomic numbers appear darker, whereas those with higher atomic numbers, e.g., iron appear brighter. There is some diffuse heterogeneity in BSE images of individual stereom trabeculae with a slightly darker region in the central part and lighter at the edge. The Mg composition of ossicles was averaged over 10 spot EDS analyses. In *Chariocrinus andreae* the Mg% range was 1.0–1.4 (average = 1.2 ± 0.13) which corresponds to ca. 5.0 mole% of $MgCO_3$. The concentration of Mg in *Balanocrinus berchteni* plate was slightly higher: 0.9–1.7 (average = 1.3 ± 0.22), which corresponds to ca. 5.3 mole% $MgCO_3$. Further evidence of the effects observed in BSE mode was provided by NanoSIMS elemental mappings and line scans taken from different regions of *C. andreae* plate (the *B. berchteni* sample was affected by strong charging thus is not shown here). The main feature of the Mg mapping and profile (Fig. 3A–C) is low Mg concentration in interstereom deposits (Mg/Ca 20–30 mmol/mol) and higher concentration in the stereom (Mg/Ca 60–70 mmol/mol) with a peak in the middle part of the trabecular bar (Mg/Ca ca. 80 mmol/ mol). Sr concentration (Fig. 3D–F) is generally very low but similarly to the Mg distribution it is lower in interstereom deposits (Sr/Ca 0.2–0.4 mmol/mol) and higher in the stereom (Sr/Ca 1.0–1.2 mmol/mol). Due to low count rate, any possible differences in Sr distribution within the stereom bar cannot be resolved.

Discussion

Complex macro- and micromorphology of the echinoderm ossicles results from precisely orchestrated biomineralization processes. Echinoderm ossicles are produced inside a syncytial membrane formed by several cells (e.g., Okazaki 1960) and a microporous structure of the stereom results directly from the 3D organization of the organic lining. There is growing evidence about a direct link between biochemical properties of some protein and glycoprotein components and modulation of the growth of the echinoderm skeleton (Ameye et al. 2001; see also review in Bottjer et al. 2006). Organic components that are present in the crystallization medium are incorporated into calcite crystals which results in their nanoporous internal structure (Robach et al. 2005, see also biomimetic experiments of Park and Meldrum 2004; Lu et al. 2005; Li and Estroff 2007). There is also growing evidence that nanocomposite structure, with nanograins 20–100 nm in size, is a universal organization of calcium carbonate biocrystals (Dauphin 2001; Cuif et al. 2004; Rousseau et al. 2005; Stolarski and Mazur 2005) and that precursor of the nanograins are amorphous calcium carbonate (ACC) granules containing high level of inorganic and organic components (Politi et al. 2004). Oaki and Imai (2006) observed the nanocomposite structure (with "nanobricks" 20–40 nm in size) in all examined echinoid stereom samples with FESEM and FETEM. Nanocomposite structure of the stereom is also supported by staining experiments with different types of organic dyes homogenously dispersed within the nanoscale architecture of the echinoid spine stereom (Oaki and Imai 2006). Examined fossil isocrinid ossicles display all micro- (stereom) and nanoscale (nanograins) details that are observed in Recent echinoderm bio-calcite hence appear not markedly affected by diagenesis. This is explained by their preservation in clay sediments and filling of their stereom pores with ferroan calcite cement that sealed off the skeleton from digenetic fluids and prevented its structural and geochemical alteration (Dickson 2004). Lack of diagenetic transformation is also supported by co-occurrence of originally calcitic (stable $CaCO_3$ polymorph) and aragonitic (metastable $CaCO_3$ polymorph) fossils in surrounding clay layers. Echinoderm ossicles from Gnaszyn seem therefore particularly suitable for geochemical studies.

Extant echinoderms produce calcite skeleton that usually contains high amount of Mg. However, it is also known that Mg content varies significantly (5–19 mol% $MgCO_3$) with physiological/environmental factors. Different skeletal parts of a single organism may contain different amount of Mg. For different taxa these values may vary as well and overall Mg content in the skeleton seems to be correlated with seawater temperature (Clarke and Wheeler 1922; Chave 1954; Weber 1969, 1973; Roux et al. 1995; Borzęcka-Prokop et al. 2007; David 1998). On the other hand, Dickson (2002, 2004) argued that Mg^{2+} composition of fossil echinoderm ossicles from "paleotropical or paleosubtropical" settings (such sample selection was made to minimize temperature effects) reflects secular changes of the seawater Mg/Ca geochemistry during the Phanerozoic. For example, Jurassic ossicles were preserved as Mg calcite with low, 4–6 mole% $MgCO_3$ content, whereas Pennsylvanian ossicles had high, 9–12 mole% $MgCO_3$ content and were preserved as calcite/microdolomite (Dickson 2004). This difference perfectly matches change between high Mg/Ca ratio of Pennsylvanian "aragonitic sea" and low Mg/Ca ratio of the Jurassic "calcitic sea".

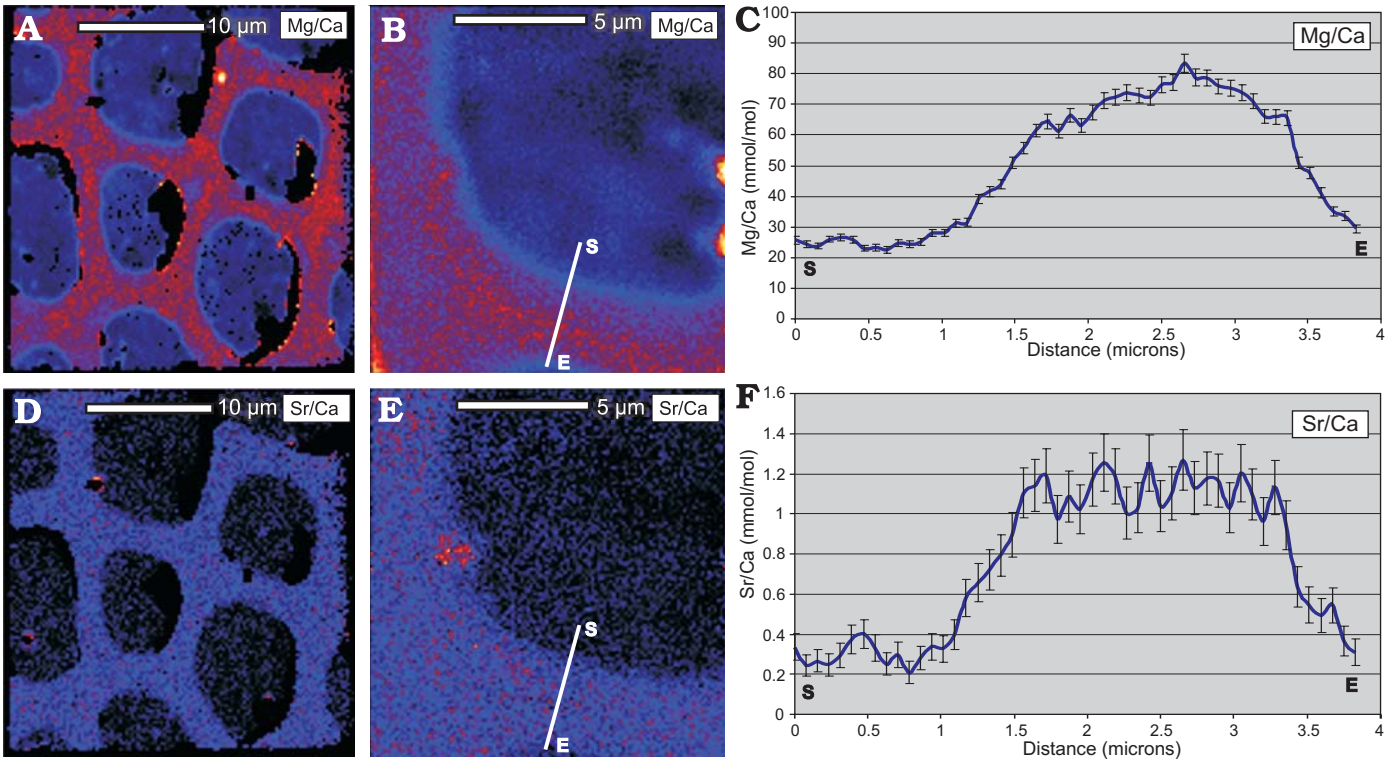

Fig. 3. Distribution of Mg/Ca and Sr/Ca in columnal plate of *Chariocrinus andreae* (Desor, 1845) from Gnaszyn clay pit, Poland (ZPAL Ca.7/1) obtained by NanoSIMS ion microprobe mapping (A, B, D, E). Line scans extracted from the images (C, F; "S" = start and "E" = end; vertical bars represent standard error). Note a sharp geochemical boundary between inter-stereom deposits and the stereom and heterogenous distribution of Mg in stereom with higher concentrations in the middle-zone of the skeletal bar. There is also clear difference between Sr content between inter-sterom deposits and stereom, however, due to low count rate, any possible differences within the stereom bar cannot be resolved.

At a glance, magnesium content in the Middle Jurassic crinoid ossicles from Gnaszyn (5.0–5.3 mole% of $MgCO_3$) match perfectly estimated effects of echinoderm Mg incorporation in low (about 1.4) Mg/Ca seawater ratio settings (Dickson 2004). However, Gnaszyn crinoids come from sediments deposited in what were probably colder settings. Based on $\delta^{18}O$ data from the calcitic belemnite rostra (possibly nectobenthic life style), Marynowski et al. (2007) and Wierzbowski and Joachimski (2007) suggested mean palaeotemperatures of 13.1°C or even 9.2°C, whereas $\delta^{18}O$ data from benthic oysters and trigoniid bivalves suggest 10.1°C and 7.4°C values, respectively. Consequently, the low magnesium content in Gnaszyn ossicles may not only be due to low Mg/Ca ratio of Middle Jurassic seawater but also due to low seawater temperatures. In fact, Dickson's (2002, 2004) conclusions regarding paleotropical or paleosubtropical settings with "temperatures probably between 20°C and 30°C" were indirect[1] and need to be verified with aid of similar stable isotopic tools. In future work we will try to address these interpretative problems using similarly well preserved crinoids from Poland and elsewhere with special focus on possible "vital effects" in Mg^{2+} incorporation and distribution between different parts of isocrinid skeleton that is known to exist in modern crinoids (David 1998).

Recent, fine scale geobiochemical mappings of echinoderm skeleton confirm that Mg is distributed heterogeneously in the stereom, reflecting strict biological biomineralization control. Robach et al. (2006: 92) found that large differences in Mg concentration in the teeth of sea urchins coincide with the distribution of aspartic acid (Asp) suggesting that macromolecules enriched in Asp control formation of very high Mg calcite. Such sub-micrometer scale biomineralization control is suggested also for the crinoid skeleton. Dickson (2004: fig. 1B, F) observed diffuse banding in stereom Mg calcite, generally with individual bands parallel to the stereom surface and suggested that "banding is similar to the concentric pattern of organic laminae (...) in modern echinoids" (Dickson 2004: 356). Our preliminary NanoSIMS mapping of the ossicle of *C. andreae* (Fig. 3A,B) shows that inner region of the stereom bar is Mg-enriched. Although the earliest phases of crinoid stereom growth have not been documented (most studies focus on anatomical and early phases of crinoid plate development, e.g., Lahaye and Jangoux 1987; Haig and Rouse in press) they probably can be compared with stereom growth in other echinoderms. In echinoids, the inner core of spine trabeculae is preferentially enriched in N-glycoproteins that are assumed to stabilize an amorphous calcium carbonate (ACC)

[1] Dickson (2002, 2004) assessed sea surface temperature of palaeo-locations, estimating their paleolatitutes (about 30% samples came from latitudes above 35° hence from intermediate subtropical/temperate climatic zone), next using Golonka et al. (1994) paleotemperature maps.

phase (see Ameye et al. 2001; review in Wilt and Ettensohn 2007). The central organic-enriched region is also similar to that described in larval echinoid spiculae (Benson et al. 1983) whose precursor phase is also ACC (Beniash et al. 1997). Surveys of the earliest growth phases of various carbonate invertebrate skeletons consistently show a link between organic and magnesium enriched first-formed regions and formation of precursory ACC skeleton phase (Aizenberg et al. 2002; Han et al. 2005; Weiner et. al. 2005; Meibom et al. 2008). We suggest herein, that Mg-enrichment in the central region of stereom bar of Jurassic *C. andreae* and diffuse stereom banding observed by Dickson (2004) may represent remains of original trace element signatures of transient ACC (compare Meibom et al. 2004 for scleractinian coral Mg-enriched banding). Further comparative studies with Recent material are planned to test this hypothesis.

Acknowledgements

Special thanks are due to Mariusz A. Salamon and Michał Zatoń (Faculty of Earth Sciences, University of Silesia, Poland) for access to material and for providing literature data on stratigraphy of Gnaszyn locality. Tomasz Baumiller (Museum of Paleontology, University of Michigan, USA) and Andrew B. Smith (Department of Palaeontology, The Natural History Museum, London) are thanked for constructive criticism, which helped improve the manuscript. The work was carried out with the financial support of Polish Ministry of Science and Higher Education, project no. N307-015733, Department of Chemistry, University of Warsaw, project BW-120000-501/68-179210, and Museum National d'Histoire Naturelle and the Agence National de la Recherche.

References

Aizenberg, J., Lambert, G., Weiner, S., and Addadi, L. 2002. Factors involved in the formation of amorphous and crystalline calcium carbonate: a study of an ascidian skeleton. *Journal of the American Chemical Society* 124: 32–39.

Ameye L., De Becker, G., Killian, C., Wilt, F., Kemps, R., Kuypers S., and Dubois, P. 2001. Proteins and saccharides of the sea urchin organic matrix of mineralization: Characterization and localization in the spine skeleton. *Journal of Structural Biology* 134: 56–66.

Beniash, E., Aizenberg, J., Addadi, L., and Weiner, S. 1997. Amorphous calcium carbonate transforms into calcite during sea urchin larval spicule growth. *Proceedings of the Royal Society, Biological Sciences* 264: 461–465.

Benson, S., Jones, E., Crise-Benson, N., and Wilt, F.H. 1983. Morphology of the organic matrix of the spicule of the sea urchin larva. *Experimental Cell Research* 148: 249–253.

Berman, A., Addadi, L., and Weiner, S. 1988. Interactions of sea-urchin skeleton macromolecules with growing calcite crystals—a study of intracrystalline proteins. *Nature* 331: 546–548.

Borzęcka-Prokop, B. Wesełucha-Birczyńska, A., and Koszowska, E. 2007. MicroRaman, PXRD, EDS and microscopic investigation of magnesium calcite biomineral phases. The case of sea urchin biominerals. *Journal of Molecular Structure* 828: 80–90.

Bottjer, D.J., Davidson, E.H., Peterson, K.J., and Cameron, R.A. 2006. Paleogenomics of echinoderms. *Science* 314: 956–960.

Chave, K. 1954. Aspects of biogeochemistry of magnesium 1. Calcareous marine organisms. *Journal of Geology* 65: 266–283.

Clarke, F.W. and Wheeler, W.C. 1922. The inorganic constituents of marine invertebrates (2nd edition). *U.S. Geological Survey Professional Papers* 124: 1–62.

Clausen, S. and Smith, A.B. 2008. Stem structure and evolution in the earliest pelmatozoan echinoderms. *Journal of Paleontology* 82: 737–748.

Cuif, J.-P., Dauphin, Y. Berthet, P., and Jegoudez, J. 2004. Associated water and organic compounds in coral skeletons: Quantitative thermogravimetry coupled to infrared absorption spectrometry. *Geochemistry, Geophysics, Geosystems* 5, Q11011, doi:10.1029/2004GC000783.

Dauphin, Y. 2001. Nanostructures de la nacre des tests de céphalopodes actuels. *Paläontologische Zeitschrift* 75: 113–122.

David, J. 1998. *Adaptation morphologique, croissance et production bioclastique chez les crinoďdes pédonculés actuels et fossiles (Pentacrines et Millericrinina). Application paléoécologique aux gisements du Jurassique supérieur des Charentes et du nord-est du bassin de Paris. Travaux Universitaires*. 551 pp. Thèse nouveau doctorat, Université de Reims, Reims, France (Université de Soutenance).

Dickson, J.A.D. 2002. Fossil echinoderms as monitor of the Mg/Ca ratio of Phanerozoic oceans. *Science* 298:1222–1224.

Dickson, J.A.D. 2004. Echinoderm skeletal preservation: calcite-aragonite seas and the Mg/Ca ratio of phanerozoic oceans. *Journal of Sedimentary Research* 74: 355–365.

Donnay, G. and Pawson, D.L. 1969. X-ray diffraction studies of echinderm plates. *Science* 166: 1147–1150.

Gedl, P., Kaim, A., Boczarowski, A., Kędzierski, M, Smoleń, J., Szczepanik, P., Witkowska, M., and Ziaja, J. 2003. Rekonstrukcja paleośrodowiska sedymentacji środkowojurajskich iłów rudonośnych Gnaszyna (Częstochowa) – wyniki wstępne. *Tomy Jurajskie* 1: 19–27.

Gedl, P., Boczarowski, A., Dudek, T., Kaim, A., Kędzierski, M., Leonowicz, P., Smoleń, J., Szczepanik, P., Witkowska, M., and Ziaja, J. 2006. Stop B1.7—Gnaszyn clay pit (Middle Bathonian–lowermost Upper Bathonian). Lithology, fossil assemblages and paleoenvironment. *7th International Congress on the Jurassic System. September 6–18 2006, Kraków, Poland,* 155–156. Polish Geological Institute, Warszawa.

Golonka, J., Ross, M.I., and Scotese, C.R. 1994. Phanerozoic paleogeographic and paleoclimatic modeling maps. *In*: A.F. Embry, B. Beauchamp, and D.J. Glass (eds.), *Pangaea: Global Environments and Resources*, 1–47. Canadian Society of Petroleum Geologists, Calgary.

Han, Y.J., Wysocki, L.M., Thanawala. M.S., Siegrist, T., and Aizenberg, J. 2005. Template-dependent morphogenesis of oriented calcite crystals in the presence of magnesium ions. *Angewandte Chemie, International Edition* 117: 2–6.

Haig, J.A. and Rouse, G.W. (in press). Larval development of the featherstar *Aporometra wilsoni* (Echinodermata: Crinoidea). *Invertebrate Biology*, doi: 10.1111/j.1744-7410.2008.00134.x.

Lahaye, M-C. and Jangoux, M. 1987. The skeleton of the stalked stages of the comatulid crinoid *Antedon bifida* (Echinodermata). Fine structure and changes during growth. *Zoomorphology* 107: 58–65.

Li, H. and Estroff, L.A. 2007. Porous calcite single crystals grown from a hydrogel medium. *CrystEngComm* 9: 1153–1155.

Lu, C., Qi, L., Cong, H., Wang, X., Yang, J., Yang, L., Zhang, D., Ma, J., and Cao, W. 2005. Synthesis of calcite single crystals with porous surface by templating of polymer latex particles. *Chemistry of Materials* 17: 5218–5224.

Majewski, W. 1997. *Amonity z iłów rudonośnych okolic Częstochowy*. 99 pp. Unpublished M.Sc. thesis, Department of Geology, University of Warsaw, Warsaw.

Majewski, W. 2000. Middle Jurassic concretions from Częstochowa (Poland) as indicators of sedimentation rates. *Acta Geologica Polonica* 50: 431–439.

Marynowski, L., Zatoń, M., Simoneit, B.R.T., Otto, A., Jędrysek, M.O, Grelowski, C., and Kurkiewicz, S. 2007. Compositions, sources and depositional environments of organic matter from the Middle Jurassic clays of Poland. *Applied Geochemistry* 22: 2456–2485.

Matyja, B.A. and Wierzbowski, A. 2000. Ammonites and stratigraphy of the uppermost Bajocian and Lower Bathonian between Częstochowa and Wieluń, Central Poland. *Acta Geologica Polonica* 50: 191–209.

Matyja, B.A. and Wierzbowski, A. 2006. Field Trip B1—Biostratigraphical framework from Bajocian to Oxfordian. Introduction. *Jurassic of Poland and adjacent Slovakian Carpathians, Fieldtrip guidebook, 7th International Congress on the Jurassic System*, 133–136. Polish Geological Institute, Warsaw.

Meibom, A., Cuif, J.P., Hillion, F., Constantz, B.R., Juillet-Leclerc, A., Dauphin, Y., Watanabe, T., and Dunbar, R.B. 2004. Distribution of magnesium in coral skeleton. *Geophysical Research Letters* 31, L23306, doi:10.1029/2004GL021313.

Meibom, A., Cuif, J.P., Houlbreque, F., Mostefaoui, S., Dauphin, Y., Meibom, K.L., and Dunbar, R. 2008. Compositional variations at ultrastructure length scales in coral skeleton. *Geochimica et Cosmochimica Acta* 72: 1555–1569.

Oaki, Y. and Imai, H. 2006. Nanoengineering in Echinoderms: The emergence of morphology from nanobricks. *Small* 1: 66–70.

Okazaki, K. 1960. Skeleton formation of sea urchin larvae. II. Organic matrix of the spicule. *Embryologia* 5: 283–320.

Park, R.J. and Meldrum, F.C. 2004. Shape-constraint as a route to calcite single crystals with complex morphologies. *Journal of Materials Chemistry* 14: 2291–2296.

Politi, Y., Arad, T., Klein, E., Weiner, S., and Addadi, L. 2004. Sea urchin spine calcite forms via a transient amorphous calcium carbonate phase. *Science* 306: 1161–1164.

Robach, J.S., Stock, S.R., and Veis, A. 2005. Transmission electron microscopy characterization of macromolecular domain cavities and microstructure of single-crystal calcite tooth plates of the sea urchin *Lytechinus variegatus*. *Journal of Structural Biology* 151: 18–29.

Robach, J.S., Stock, S.R., and Veis, A. 2006. Mapping of magnesium and of different protein fragments in sea urchin teeth via secondary ion mass spectroscopy. *Journal of Structural Biology* 155: 87–95.

Rousseau, M., Lopez, E., Stempflé, P., Brendlé, M., Franke, L., Guette, A., Naslain, R., and Bourrat, X. 2005. Multiscale structure of sheet nacre. *Biomaterials* 26: 6254–6262.

Roux, M. 1975. Microstructural analysis of the crinoid stem. *The University of Kansas, Palaeontological Contributions* 75: 1–7.

Roux, M., Renard, M., Ameziane-Cominardi, N., and Emmanuel, L. 1995. Zoobathymétrie et composition chimique de la calcite des ossicules du pédoncule des crinoïdes. *Comptes rendus de l'Académie des sciences Paris, série II a* 321: 675–680.

Salamon, M.A. and Zatoń, M. 2007. A diverse crinoid fauna from the Middle Jurassic (Upper Bajocian–Callovian) of the Polish Jura Chain and Holy Cross Mountains (south-central Poland). *Swiss Journal of Geosciences* 100: 153–164.

Stolarski, J. and Mazur, M. 2005. Nanostructure of biogenic versus abiogenic calcium carbonate crystals. *Acta Palaeontologica Polonica* 50: 847–865.

Weber, J.N. 1969. The incorporation of magnesium into the skeletal calcites of echinoderms. *American Journal of Science* 267: 537–566.

Weber, J.N. 1973. Temperature dependence of magnesium in echinoid and asteroid skeletal calcite: a reinterpretation of its significance. *Journal of Geology* 81: 543–556.

Weiner, S. 1985. Organic matrix-like macromolecules associated with the mineral phase of sea-urchin skeletal plates and teeth. *Journal of Experimental Zoology* 234: 7–15.

Weiner, S., Sagi, I., and Addadi, L. 2005. Choosing the crystallization path less traveled. *Science* 309: 1027–1028.

Wierzbowski, H. and Joachimski, M. 2007. Reconstruction of late Bajocian–Bathonian marine palaeoenvironments using carbon and oxygen isotope ratios of calcareous fossils from the Polish Jura Chain (central Poland). *Palaeogeography, Palaeoclimatology, Palaeoecology* 254: 523–540.

Wilt, F.H. 1999. Matrix and mineral in the sea urchin larval skeleton. *Journal of Structural Biology* 126: 216–226.

Wilt, F.H. and Ettensohn, C.E. 2007. Morphogenesis and biomineralization of the sea urchin larval endoskeleton. *In*: E. Bauerlein (ed.), *Handbook of Biomineralization*, 183–210. Wiley-VCH, Winheim.

Zatoń, M., Barbacka, M., Marynowski, L., and Krzystanek, J. 2006. *Sagenopteris* (Caytoniales) with its possible preserved biomarkers from the Bathonian of the Polish Jura, south-central Poland. *Neues Jahrbuch fur Geologie und Palaontologie*, *Monatschefte* 7: 385–402.